ARTICLES

Structural Characteristics and Reactivity/Reducibility Properties of Dispersed and Bilayered $V_2O_5/TiO_2/SiO_2$ Catalysts

Xingtao Gao,[†,‡] Simon R. Bare,[§,||] J. L. G. Fierro,[⊥] and Israel E. Wachs*[,†]

Department of Chemistry and Chemical Engineering, Zettlemoyer Center for Surface Studies, Lehigh University, 7 Asa Drive, Bethlehem, Pennsylvania 18015, UOP Research, Des Plaines, Illinois 60017, and Institute de Catalisis y Petroleoquimica, C.S.I.C., Campus Univeritario Cantoblanco, E-28049-Madrid, Spain

Received: August 12, 1998; In Final Form: October 28, 1998

Dispersed and bilayered $V_2O_5/TiO_2/SiO_2$ catalysts were successfully synthesized by the incipient wetness impregnation method, and their surface structures under various conditions were extensively investigated by combined in situ Raman, UV−vis−NIR diffuse reflectance and X-ray absorption near-edge spectroscopies, as well as X-ray photoelectron spectroscopy. Temperature-programmed reduction and methanol oxidation were employed as chemical probe reactions to examine the reducibility and reactivity/selectivity of these catalysts. The spectroscopic results revealed that both vanadium oxide and titanium oxide on SiO_2 are dispersed as two-dimensional metal oxide overlayers. The surface vanadium oxide species on the dispersed TiO_2/SiO_2 are predominantly isolated VO_4 units [O═V(O−support)$_3$] in the dehydrated state and become polymerized VO_5/VO_6 units upon hydration. The surface vanadium oxide species preferentially interact with the surface titanium oxide species on silica, and the V(V) cations possess oxygenated ligands of Si(IV)−O$^-$ and Ti(IV)−O$^-$ in the O═V(O−support)$_3$ unit with varying ratios from 3:0 to 0:3, which depends on the vanadia and titania loadings. The varying ratio of the Si(IV)−O$^-$ and Ti(IV)−O$^-$ oxygenated ligands significantly affects the chemical properties of the isolated VO_4 units. Consequently, the reducibility of the surface vanadium oxide species is altered and the reduction occurs over a wider temperature range. In addition, the methanol oxidation turn-over frequency of the surface VO_4 species on TiO_2/SiO_2 increases an order of magnitude relative to V_2O_5/SiO_2. Thus, the oxygenated ligands around the V cations play a critical role in determining the reactivity of the surface vanadium oxide species on the oxide supports.

Introduction

The TiO_2/SiO_2 support has been considered as an advanced support material to replace pure TiO_2, since it possesses enhanced thermal/mechanical stability, high surface area and is economically attractive. Much attention has been paid to the $V_2O_5/TiO_2/SiO_2$ catalyst system due to its excellent catalytic performance in the SCR (selective catalytic reduction) of nitrogen oxides with ammonia (high activity/selectivity, high surface area and high resistance to sintering).[1−5] Additional reactions have also been examined using the $V_2O_5/TiO_2/SiO_2$ catalysts, including NO reduction with CO,[6] selective oxidation reactions of toluene,[7] *o*-xylene,[8a] and ethanol.[8b] These studies mostly focused on the catalytic properties of $V_2O_5/TiO_2/SiO_2$ catalysts[2,4−8] in an effort to find the catalysts with improved catalytic performances (i.e., high surface area, excellent thermal stability/mechanical strength, and a catalytic property comparable to that of the V_2O_5/TiO_2 catalyst). For many of the $V_2O_5/TiO_2/SiO_2$ catalysts intended for industrial applications,[1,2,4−6,8] the vanadium oxide was most likely dispersed on the crystalline titania particles present on silica because titania loadings were usually high and the catalytic properties (activity/selectivity) of the catalysts were very similar to that of V_2O_5/TiO_2 catalysts. However, very little or no molecular structural characterization was provided about the $V_2O_5/TiO_2/SiO_2$ systems.

Only a few studies[3,9] were intended to prepare dispersed $V_2O_5/TiO_2/SiO_2$ catalysts and to study the corresponding structural characteristics in order to understand the catalytic behavior of the $V_2O_5/TiO_2/SiO_2$ catalysts. Rajadhyaksha et al.[3] investigated a series of 7% $V_2O_5/TiO_2/SiO_2$ catalysts with the titanium oxide content varying from 8% to 34% TiO_2. However, even for the sample with the lowest TiO_2 loading a Raman band at ∼145 cm^{-1} due to crystalline TiO_2 (anatase) was still observed, which indicates the presence of some TiO_2 crystallites on silica. Lapina et al.[9] studied the surface complexes of the hydrated and dehydrated $V_2O_5/TiO_2/SiO_2$ catalysts by ^{51}V and ^{1}H high-resolution solid-state NMR spectroscopy, which provides information only on the coordination geometry of the V atoms. Different types of vanadium oxide complexes, with either octahedral or tetrahedral coordination, were detected in the dehydrated state. It was proposed that two types of mixed

* To whom correspondence should be addressed. E-mail: iew0@lehigh.edu.
[†] Lehigh University.
[‡] E-mail: xig2@lehigh.edu.
[§] UOP Research.
[||] E-mail: srbare@uop.com.
[⊥] Campus Univeritario Cantoblanco.

10.1021/jp983357m CCC: $18.00
Published on Web 01/08/1999

V−Ti−Si oxide complexes are present on silica, where V atoms are located either in highly distorted or in regular tetrahedral environments depending on the sequence of vanadia and titania deposition. However, no other characterization techniques were employed in this study to determine the dispersion of titanium oxide and vanadium oxide on silica. Therefore, a fundamental molecular-level understanding of the interaction between dispersed surface titanium oxide and surface vanadium oxide species on silica has not been achieved because of the lack of systematic structural characterization studies as well as the unsuccessful synthesis of dispersed $V_2O_5/TiO_2/SiO_2$ catalysts.

Investigation of dispersed $V_2O_5/TiO_2/SiO_2$ catalysts at the molecular level is critical to understanding the interfacial interactions between surface layers and the catalytic properties of surface metal oxides. In the present investigation, dispersed $V_2O_5/TiO_2/SiO_2$ catalysts with various V/Ti atomic ratios were prepared. The presence of surface titanium oxide and vanadium oxide species was confirmed with different characterization techniques. In situ studies of the molecular structures of dispersed $V_2O_5/TiO_2/SiO_2$ catalysts under various environmental conditions were performed with Raman spectroscopy, X-ray photoelectron spectroscopy (XPS), UV−vis−NIR diffuse reflectance spectroscopy (DRS), and X-ray absorption near-edge-structure (XANES) spectroscopy. Temperature-programmed reduction (TPR) and methanol oxidation as chemical reaction probes were employed to examine the redox property and catalytic reactivity/selectivity properties of these dispersed $V_2O_5/TiO_2/SiO_2$ catalysts, respectively. Thus, the structural characterization data and the corresponding reactivity/selectivity results will allow us to establish the molecular structure−reactivity/selectivity relationships for this catalyst system.

Experimental Section

1. Catalyst Preparation. The SiO_2 support used for this study was Cabosil EH-5 (S_{BET} = 332 m^2/g), and the TiO_2 support was Degussa P-25 (S_{BET} = 45 m^2/g). The preparation of the TiO_2/SiO_2 supported oxides has been described in detail elsewhere.[10] The dispersed $V_2O_5/TiO_2/SiO_2$ catalysts were prepared by the incipient-wetness impregnation of 2-propanol solutions of vanadium isopropoxide ($VO(O-Pr^i)_3$, Alfa-Aesar 97% purity) with various supports. The preparation was performed inside a glovebox with continuously flowing N_2. The supports were initially dried at 120 °C to remove the physisorbed water before impregnation. After impregnation, the samples were kept inside the glovebox overnight. The samples were subsequently dried in flowing N_2 at 120 °C for 1 h and 300 °C for 1 h. Then, the $V_2O_5/TiO_2/SiO_2$ samples were calcined in flowing air at 300 °C for 1 h and 500 °C for 2 h, while the V_2O_5/SiO_2 and V_2O_5/TiO_2 samples were calcined in flowing air at 300 °C for 1 h and 450 °C for 2 h. The element analysis of the $V_2O_5/TiO_2/SiO_2$ catalysts was accomplished by inductively coupled plasma (ICP).

The BET surface area of each sample was determined by nitrogen adsorption/desorption isotherms on a Micromeritics ASAP 2000.

2. Raman Spectroscopy. The Raman spectra were obtained with the 514.5 nm line of an Ar^+ ion laser (Spectra Physics, model 164). The scattered radiation from the sample was directed into an OMA III (Princeton Applied Research, model 1463) optical multichannel analyzer with a photodiode array cooled thermoelectrically to −35 °C. The samples were pressed into self-supporting wafers. The Raman spectra of the hydrated samples were obtained during rotation of the sample under ambient conditions. The Raman spectra of the dehydrated samples were recorded at room temperature after heating the sample in flowing O_2 at 450−500 °C for 1 h in a stationary quartz cell.

The in situ Raman spectra during methanol oxidation were collected on a second Raman apparatus (same as above). A self-supporting sample disk of 100−200 mg was mounted on the sample holder, which is capable of spinning inside a quartz cell. The in situ Raman cell setup was described in detail elsewhere.[11] The sample was heated at 500 °C for 1 h in a flowing O_2/He mixture. The background Raman spectrum was taken after the sample was cooled to 230 °C. Then, methanol vapor was introduced by passing the He/O_2 (11/6) mixture through liquid methanol in an ice bath (4 mol % CH_3OH in the saturated gaseous mixture). The Raman spectra under reaction conditions were obtained after reaching steady state (∼30 min at 230 °C). The Raman spectra after removal of methanol from the feed stream as well as at higher temperatures of 300 and 360 °C, with/without methanol in the feed gas, were also recorded.

3. X-ray Photoelectron Spectroscopy (XPS). XPS spectra were collected with a Fisons ESCALAB 200R electron spectrometer equipped with a hemispherical electron analyzer and a Mg Kα X-ray source ($h\nu$ = 1253.6 eV) powered at 120 W. The samples were placed in small copper cylinders and mounted on a transfer rod placed in the pretreatment chamber of the instrument. All samples were outgassed at 200 °C before XPS analysis. The binding energies (BE) were referenced to Si 2p (BE = 103.4 eV) with an accuracy of ±0.2 eV. The atomic concentration ratios were calculated by correcting the intensity ratios with theoretical sensitivity factors, i.e., 1.20 for Ti $2p_{3/2}$, 1.30 for V $2p_{3/2}$, and 0.27 for Si 2p.

4. UV−Vis−NIR Diffuse Reflectance Spectroscopy (DRS). DRS spectra in the range 200−2200 nm were taken on a Varian Cary 5 UV−vis−NIR spectrophotometer. The spectra were recorded against a halon white reflectance standard as the baseline. The computer processing of the spectra with Bio-Rad Win-IR software consisted of calculation of the Kubelka−Munk function ($F(R_\infty)$) from the absorbance. The band-gap energy (E_g) for allowed transitions was determined by finding the intercept of the straight line in the low-energy rise of a plot of $[F(R_\infty) \times h\nu]^2$ against $h\nu$, where $h\nu$ is the incident photon energy.[12] Samples were loaded in a quartz flow cell with a Suprasil window. After each treatment, the quartz cell was quickly sealed and cooled to room temperature for DRS measurements. The spectra of the hydrated samples were obtained under ambient conditions, and the spectra of the dehydrated samples were obtained after samples were calcined at 500 °C in flowing O_2/He for 1 h.

5. X-ray Absorption Spectroscopy (XANES). The X-ray absorption experiments at the Ti and V K-edges were performed on beam line X19A at the National Synchrotron Light Source, Brookhaven National Laboratory. The storage ring operated at 2.5 GeV with a current between 200 and 300 mA. The samples were prepared by grinding each to fine powder and pressing into self-supporting wafers of appropriate thickness. These wafers were held in a quartz in situ XAFS cell with Kapton windows. XANES spectra were initially acquired at room temperature in a He purge and after heating to 500 °C at 10 °C /min in O_2/He (20/80), holding for 30 min at 500 °C, then cooling to room temperature.

The XANES spectra were processed using the BAN software package. The energy scale for titanium oxide was established by setting the maximum of the first derivative of the XANES spectra of the Ti metal foil to 0.0 eV. The energy scale for vanadium oxide was established by setting the first inflection

TABLE 1: Surface Areas and Compositions of $V_2O_5/TiO_2/SiO_2$ Catalysts

catalyst	surface area (m^2/g)	wt % V_2O_5[a]	bulk V/Ti atomic ratio[b]	XPS surf. V/Ti atomic ratio
5% TiO_2/SiO_2	280	0.00	0.000	0.000
1% V_2O_5/5% TiO_2/SiO_2	257	0.70	0.094	
5% V_2O_5/5% TiO_2/SiO_2	174	3.80	0.527	
10% V_2O_5/5% TiO_2/SiO_2	182	8.70	1.27	
8% TiO_2/SiO_2	253	0.00	0.000	0.000
5% V_2O_5/8% TiO_2/SiO_2	211	4.74	0.444	0.230
10% V_2O_5/8% TiO_2/SiO_2	178	8.20	0.797	0.923
10% TiO_2/SiO_2	270	0.00	0.000	0.000
5% V_2O_5/10% TiO_2/SiO_2	224	4.78	0.408	0.351
10% V_2O_5/10% TiO_2/SiO_2	194	8.50	0.756	0.893
12% TiO_2/SiO_2	265	0.00	0.00	0.000
1% V_2O_5/12% TiO_2/SiO_2	250	1.15	0.069	
5% V_2O_5/12% TiO_2/SiO_2	225	4.90	0.307	0.375
10% V_2O_5/12% TiO_2/SiO_2	181	8.70	0.567	0.557
15% TiO_2/SiO_2	229	0.00	0.000	0.000
5% V_2O_5/15% TiO_2/SiO_2	189	4.51	0.264	0.250
10% V_2O_5/15% TiO_2/SiO_2	160	8.50	0.520	0.575

[a] Actual concentration obtained by inductively coupled plasma (ICP). [b] TiO_2 concentrations of the initial TiO_2/SiO_2 supports are provided in ref 10.

point of the vanadium metal in the derivation spectrum at 5465.0 eV to zero. The spectra were normalized to unity absorption by dividing by a least-squares fit of the absorption between 50 and 250 eV above the absorption edge.

6. Temperature-Programmed Reduction (TPR). TPR was carried out with an AMI-100 system (Zeton Altamira Instruments). The catalyst sample (~60 mg) was loaded in an U-type quartz tube and pretreated at 500 °C in flowing dry air for 1 h. After cooling in an Ar flow down to 150 °C, the Ar gas was switched to a 10% H_2/Ar gas mixture. The temperature was then ramped from 150 to 700 °C with a constant heating rate of 10 °C in 10% H_2/Ar with a flow rate of 30 mL/min. After the first TPR run, some reduced samples were then reoxidized at 500 °C in flowing dry air for 1 h, and the reoxidized samples were used for the second TPR run in order to examine the stability of the catalyst sample during the redox cycle. An on-line TCD detector was used to record the H_2 consumption, and CuO was used to verify the calibration of the instrument (the experimental error is within 10%).

7. Methanol Oxidation. Methanol oxidation was used to examine the catalytic reactivity/selectivity of $V_2O_5/TiO_2/SiO_2$ catalysts. The reaction was carried out in an isothermal fixed-bed differential reactor. About 60 mg of catalyst with a size fraction of 60−100 mesh was tested for methanol oxidation at various temperatures at atmospheric pressure. The reactant gas mixture of CH_3OH/O_2/He, molar ratio of ~6/13/81, was used with a total flow rate of 100 mL/min. Analysis of the reactor effluent was performed using an on-line gas chromatograph (HP 5890 series II) equipped with FID and TCD detectors. A Carboxene-1000 packed column and a CP-sil 5CB capillary column were used in parallel for TCD and FID, respectively. The samples were pretreated in a stream of O_2/He gas mixture at 450 °C for 0.5 h before each run, and the methanol conversion data were obtained for catalytic runs within 2 h.

Results

1. Bulk Compositions and Surface Areas of $V_2O_5/TiO_2/SiO_2$ Catalysts. The nominal and actual bulk compositions as well as surface areas of the $V_2O_5/TiO_2/SiO_2$ samples are shown in Table 1. The nominal values are in good agreement with the actual values, considering the experimental errors in both preparation and element analysis. Therefore, all the vanadia and titania loadings mentioned in the paper are referred to the nominal values, and the nominal values were used to calculate the H_2 consumption for TPR and TOF (turn-over frequency) for methanol oxidation. However, the bulk V/Ti atomic ratios are calculated from the actual concentrations of titania and vanadia on silica. The surface areas of the $V_2O_5/TiO_2/SiO_2$ catalysts generally decrease with increasing vanadia and titania loadings.

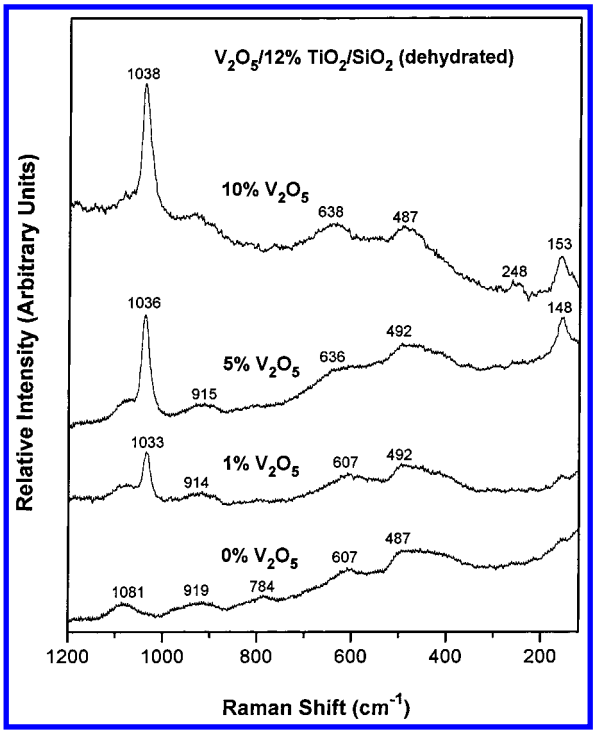

Figure 1. Raman spectra of the dehydrated V_2O_5/12% TiO_2/SiO_2 samples.

2. XPS Surface Analysis. The surface V/Ti atomic ratios of some of the $V_2O_5/TiO_2/SiO_2$ catalysts obtained by XPS analysis are also listed in Table 1. The surface V/Ti ratios are relatively consistent with the bulk V/Ti ratios, within experimental error, indicating that both vanadium oxide and titanium oxide species are dispersed on silica. With the BE value of Si 2p being taken as the reference (103.4 eV), the BE value of Ti $2p_{3/2}$ for most of the $V_2O_5/TiO_2/SiO_2$ catalysts listed in Table 1 is almost constant (459.2 eV) and is higher than the BE of pure TiO_2 (458.5 eV).

3. Raman Spectroscopy. The Raman spectra of TiO_2/SiO_2 samples were previously reported.[10] The results indicate that the 12% TiO_2/SiO_2 sample corresponds to approximately experimental monolayer coverage (the actual TiO_2 loading in this sample is 14.75 wt %). Above monolayer coverage, TiO_2 crystallites (anatase) are formed on the silica surface as indicated by a Raman band at 154 cm^{-1}. However, large TiO_2 particles (>40 Å), which are detectable by XRD measurements, can only be observed above 30% TiO_2 loading.

The Raman spectra of the dehydrated 0%−10% V_2O_5/12% TiO_2/SiO_2 samples are presented in Figure 1. The 12% TiO_2/SiO_2 support possesses Raman features at ~410, ~487, 607, 784, ~919, and 1081 cm^{-1}. The broad bands at 784, 607, 487, and ~410 cm^{-1} are due to SiO_2, and two bands at ~1080 and ~919 cm^{-1} are associated with perturbed silica vibrations that are indicative of the formation of Ti−O−Si bonds.[10] A strong band at 1033−1038 cm^{-1} due to the V=O stretching vibration

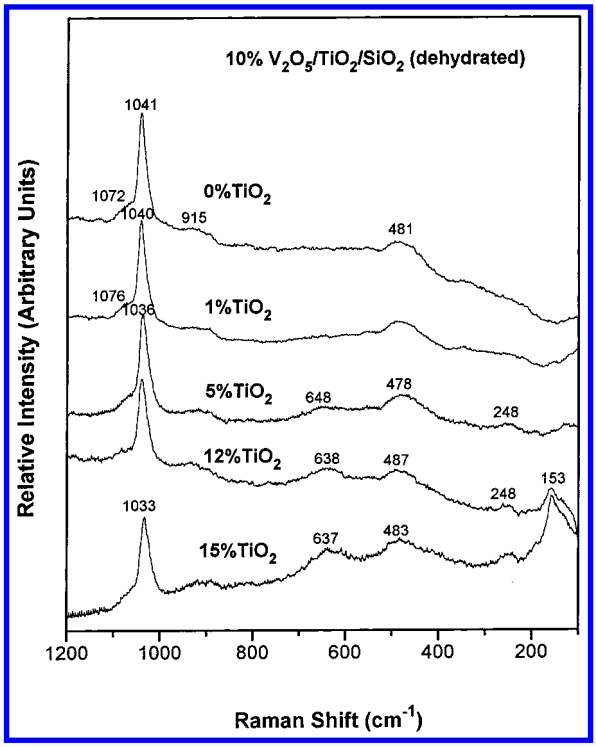

Figure 2. Raman spectra of the dehydrated 10% $V_2O_5/TiO_2/SiO_2$ samples.

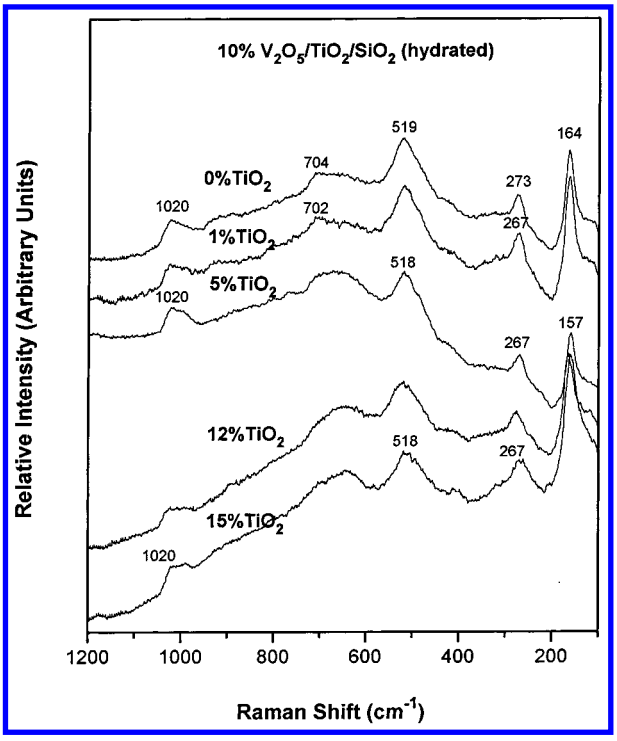

Figure 3. Raman spectra of the hydrated 10% $V_2O_5/TiO_2/SiO_2$ samples.

appears with the addition of vanadium oxide. Unlike the dehydrated, dispersed V_2O_5/SiO_2 samples whose V═O vibration is independent of vanadia loading,[13] decreasing the vanadia loading on TiO_2/SiO_2 supports shifts the V═O vibration to lower wavenumbers. The 607 cm^{-1} band, due to the three-member siloxane rings, decreases with increasing vanadia loading, indicating that the silica surface covered with the surface titanium oxide species also interacts with the surface vanadium oxide species. Simultaneously, two new broad bands appear at ∼638 and ∼248 cm^{-1} (see below for assignment of these bands). A Raman band at ∼150 cm^{-1} due to a small amount of TiO_2 crystallites appears at a vanadia loading of 5% V_2O_5 and above, indicating that the deposition of vanadium oxide on 12% TiO_2/SiO_2 may cause slight aggregation of the surface titanium oxide species.

The Raman spectra of the dehydrated 10% V_2O_5 on 0%−15% TiO_2/SiO_2 supports are compared in Figure 2. No V_2O_5 crystallites are detected in these samples, since no Raman bands appear at 994, 697, 284, and 144 cm^{-1} due to crystalline V_2O_5. The dehydrated 10% V_2O_5/SiO_2 sample possesses a Raman band at 1041 cm^{-1} from the terminal V═O vibration of the isolated VO_4 species and bands at 1072, 915, and 481 cm^{-1} due to silica vibrations.[13] Increasing the TiO_2 loading generally shifts the V═O stretching vibration to lower wavenumbers, suggesting a higher degree of interaction between dispersed vanadium oxide species and titanium oxide species on silica. The two new bands at 648−637 and ∼248 cm^{-1} appear at high concentrations of dispersed vanadium and titanium oxides. These two bands are not associated with the TiO_2 crystallites (anatase) originating from the slight aggregation of surface titanium oxide, since for the 5% V_2O_5/5% TiO_2/SiO_2 sample these two bands are observed without the presence of the ∼150 cm^{-1} band due to crystalline TiO_2. These two bands appear to be associated with both surface vanadium oxide species and surface titanium oxide species. Therefore, the two new Raman bands at 648−637 and ∼248 cm^{-1} could be temporarily assigned to the stretching and bending modes of V−O−Ti bridging bonds between the surface vanadium oxide species and titanium oxide species (e.g., O═V(−O−Ti−O−Si) complexes), respectively, because a V−O−Ti bond with a bond order of ∼1 should exhibit a Raman band at ∼650 cm^{-1}.[15]

A weak and broad Raman band centered at ∼915 cm^{-1} is observed on all these 10% $V_2O_5/TiO_2/SiO_2$ samples (Figure 2). For the 10% V_2O_5/SiO_2 sample, the weak ∼915 cm^{-1} band has previously been attributed to silica functionalities.[13] For the V_2O_5/TiO_2 samples, a broad Raman band observed at 940−915 cm^{-1} has been assigned to polymerized surface vanadium oxide species, and its relative intensity increases with increasing vanadia loading.[14] Therefore, the ∼915 cm^{-1} Raman band for the $V_2O_5/TiO_2/SiO_2$ samples most likely originates from silica functionalities because its intensity is relatively very weak and does not noticeably change with titania loading from 0% to 15% TiO_2. These results also suggest that the dehydrated surface VO_x species on 0%−15% TiO_2/SiO_2 supports are predominately isolated VO_4 species.

The Raman spectra of the hydrated 10% V_2O_5 on 0%−15% TiO_2/SiO_2 supports are presented in Figure 3. All these Raman spectra are similar except for slight intensity differences in the 704−650 cm^{-1} region. For the hydrated 10% V_2O_5/SiO_2 catalyst, the Raman bands at ∼1020, 704−650, ∼518, 273−264, and 164−155 cm^{-1} have been assigned to 2D polymerized VO_5/VO_6 species.[13] Comparison of the hydrated spectra shown in Figure 3 suggests that the hydrated 2D polymerized VO_5/VO_6 species are also dominant on the TiO_2/SiO_2 supports. The 2D polymerized VO_5/VO_6 species appear to be characteristic of hydrated surface vanadium oxide species on silica as well as surface titanium oxide species modified silica.

The in situ Raman spectra of the 10% V_2O_5/12% TiO_2/SiO_2 sample during methanol oxidation as a function of temperature and feed gas composition are presented in Figure 4. The introduction of methanol in the feed stream dramatically reduces the 1037 cm^{-1} band due to the isolated VO_4 species. Instead, a weak Raman band appears at 1029 cm^{-1}, which may be due to the V═O stretching vibration of some unreacted surface V(V) species. In the corresponding 2700−3100 region, no C−H

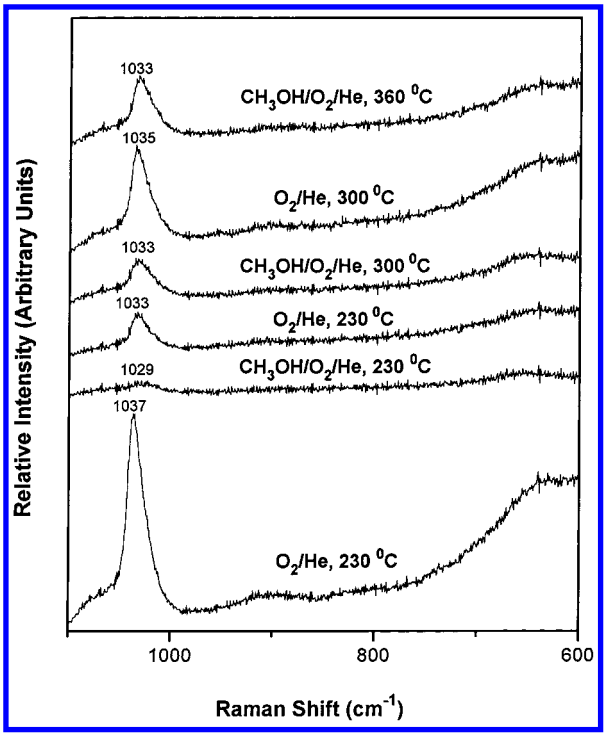

Figure 4. In situ Raman spectra of the 10% V_2O_5/12% TiO_2/SiO_2 catalyst during methanol oxidation.

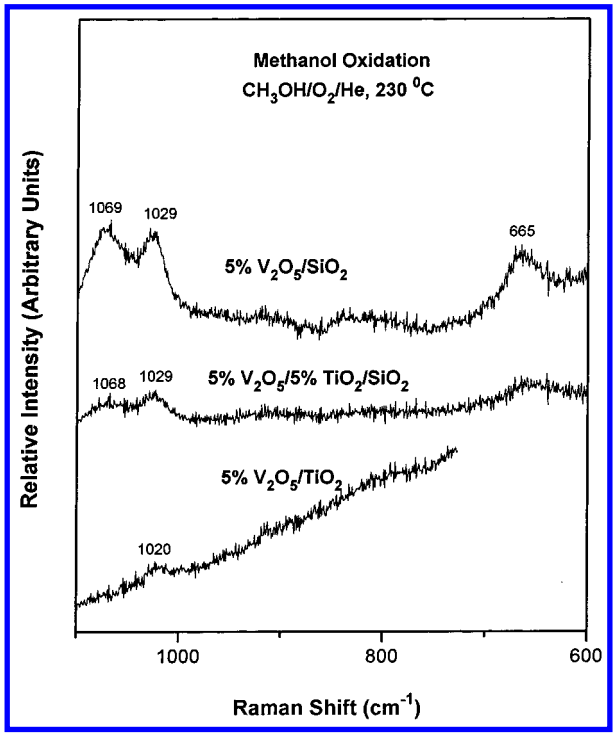

Figure 5. Comparison of in situ Raman spectra of 5% V_2O_5 on SiO_2, 5% TiO_2/SiO_2, and TiO_2 supports during methanol oxidation at 230 °C.

vibrations are detected (not shown here). The removal of methanol from the feed stream partially regenerates the ~1037 cm^{-1} band due to the isolated VO_4 species.

The in situ Raman spectra of the 5% V_2O_5/SiO_2, 5% V_2O_5/TiO_2, and 5% V_2O_5/5% TiO_2/SiO_2 catalysts during methanol oxidation at 230 °C are compared in Figure 5. As previously discussed,[13] the surface V−methoxy complexes on silica exhibit three Raman bands at 1069, 1029, and 665 cm^{-1} due to the C−O stretching, V═O stretching, and C−O bending modes,

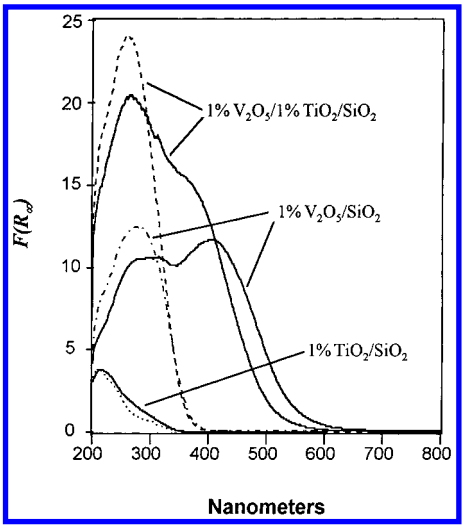

Figure 6. UV−vis DRS spectra of the hydrated (solid lines) and dehydrated (dash lines) samples.

respectively. In contrast, only a very weak Raman band at ~1020 cm^{-1} is observed for the 5% V_2O_5/TiO_2 catalyst, which may be due to the V═O stretching vibration of some unreacted V(V) species. The Raman band at 1029 cm^{-1}, due to isolated VO_4 species, and a broad band at 940−915 cm^{-1}, due to polymerized vanadium oxide species on titania,[14] almost completely disappear during methanol oxidation. These results suggest that either the surface vanadium oxide species on titania is in a highly reduced state or the surface vanadium oxide species form some kind of complex with chemisorbed methanol molecules that are undetectable by Raman spectroscopy (e.g., highly polarized, ionic V−methoxy complexes that are Raman inactive or very poor Raman scatterers). The latter case is more likely, since the V−methoxy complexes are readily observed by in situ FT-IR spectroscopy during methanol oxidation.[16] Therefore, the surface V−methoxy species on titania are somehow different from the surface V−methoxy species on silica.

The addition of 5% TiO_2 as surface titanium oxide species to silica significantly weakens the three bands due to the silica-like surface V−methoxy complexes, and the relative intensity of the ~1029 cm^{-1} band appears to be higher than the 1068 cm^{-1} band (see Figure 5), suggesting that the TiO_2/SiO_2 surface is dominated by the titania-coordinated surface V−methoxy complexes. These results indicate that during methanol oxidation, the surface vanadium oxide species on the TiO_2/SiO_2 supports behave more like that on the TiO_2 support than on the SiO_2 support, suggesting that the surface vanadium oxide species are predominantly coordinated to the surface titanium oxide species on silica.

4. UV−Vis−NIR Diffuse Reflectance Spectroscopy. The UV−vis DRS spectra of 1% V_2O_5/1% TiO_2/SiO_2 and 10% V_2O_5/12% TiO_2/SiO_2 samples under hydrated and dehydrated conditions are compared with TiO_2/SiO_2 and V_2O_5/SiO_2 at the same loadings in Figures 6 and 7. The corresponding band maxima and band-gap energies are provided in Table 2. The band maxima and edge energies of the 5% V_2O_5/5% TiO_2/SiO_2 and the 10% V_2O_5/5% TiO_2/SiO_2 samples under hydrated and dehydrated conditions are also listed in Table 2. All the dehydrated $V_2O_5/TiO_2/SiO_2$ samples exhibit only one ligand-to-metal charge transfer (LMCT) band, which apparently originates from the overlapped LMCT transitions of both V and Ti cations (electronic transitions from orbitals mainly consisting of oxygen 2p orbitals to vanadium/titanium 3d orbitals). Notably,

TABLE 2: Band Maxima and Edge Energies of the Hydrated and Dehydrated Samples

samples	band max (nm) (dehydr)	E_g (eV) (dehydr)	band max (nm) (hydr)	E_g (eV) (hydr)
1% TiO_2/SiO_2	210 (47 600 cm^{-1})	4.68	215 (46 600 cm^{-1})	4.66
5% TiO_2/SiO_2	248 (40 400 cm^{-1})	4.19	262 (38 200 cm^{-1})	3.88
12% TiO_2/SiO_2	258 (38 800 cm^{-1})	3.84	269 (37 200 cm^{-1})	3.78
1% V_2O_5/SiO_2	278 (36 000 cm^{-1})	3.6	283, 426 (35 300, 23 500 cm^{-1})	2.5
5% V_2O_5/SiO_2	286 (34 700 cm^{-1})	3.5	285, 433 (35 000, 23 000 cm^{-1})	2.4
10% V_2O_5/SiO_2	296 (33 700 cm^{-1})	3.4	278, 436 (34 400, 24 400 cm^{-1})	2.4
1% V_2O_5/1% TiO_2/SiO_2	260 (38 500 cm^{-1})	3.8	264, 393 (37 900, 25 400 cm^{-1})	2.7
5% V_2O_5/5% TiO_2/SiO_2	268 (37 300 cm^{-1})	3.5	271, 424 (36 900, 23 600 cm^{-1})	2.7
10% V_2O_5/5% TiO_2/SiO_2	276 (36 200 cm^{-1})	3.5	270, 420 (39 800, 25 000 cm^{-1})	2.6
10% V_2O_5/12% TiO_2/SiO_2	270 (37 000 cm^{-1})	3.4	269, 423 (37 200, 23 600 cm^{-1})	2.6

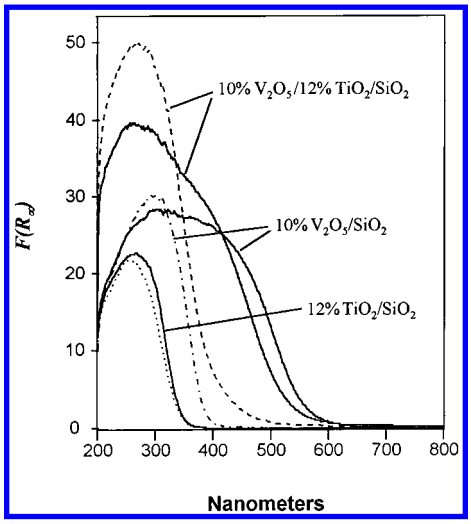

Figure 7. UV−vis DRS spectra of the hydrated (solid lines) and dehydrated (dash lines) samples.

TABLE 3: Energy Positions of the Pre-edge Peak and the Edge in the V K-Edge XANES Spectra of the 10% V_2O_5/SiO_2 and 10% V_2O_5/15% TiO_2/SiO_2 Samples

sample	pre-peak position (eV)	pre-peak height	edge (eV)[a]
10% V_2O_5/SiO_2 (hydr)	6.0	0.51	ill defined
10% V_2O_5/15% TiO_2/SiO_2 (hydr)	6.0	0.52	ill defined
10% V_2O_5/SiO_2 (dehy)	5.8	0.64	18.8
10% V_2O_5/15% TiO_2/SiO_2 (dehy)	5.9	0.60	18.8

[a] Determined from the second maximum of the derivative XANES spectra.

the LMCT band of the dehydrated V_2O_5/SiO_2 sample is significantly stronger than the corresponding dehydrated TiO_2/SiO_2 support with a similar loading. Moreover, as shown in Table 3, the band edge position of the dehydrated vanadium oxide species is significantly lower than that of the surface titanium oxide species. Thus, the edge energies of the LMCT transitions for the dehydrated, dispersed $V_2O_5/TiO_2/SiO_2$ samples should be mainly determined by the edge energies of V(V) cations. As shown in Table 2, the edge energies of these dehydrated $V_2O_5/TiO_2/SiO_2$ samples are similar to those of the dehydrated V_2O_5/SiO_2 samples. It was previously concluded[13] that for the dispersed V_2O_5/SiO_2 catalysts, the dehydrated vanadium oxide species consist of isolated VO_4 units. Therefore, for the dispersed $V_2O_5/TiO_2/SiO_2$ samples, the dehydrated surface vanadium oxide species must also predominantly consist of isolated VO_4 species on the TiO_2/SiO_2 surface (in agreement with the Raman results). It is noted that the LMCT transitions for the dehydrated 1%−10% V_2O_5/SiO_2 and 1% V_2O_5/1% TiO_2/SiO_2 samples occur below 400 nm. However, for the samples with higher vanadia and titania loadings, such as the dehydrated 10% V_2O_5/12% TiO_2/SiO_2 sample shown in Figure 7, some LMCT transitions occur above 400 nm, as can be seen from the tail of the main absorption peak at 270 nm. This low-energy absorption tail might be due to a small amount of polymerized surface vanadium oxide species or due to the synergistic effect when the isolated V cations bind with polymerized Ti cations. Thus, the DRS experiments cannot exclude the presence of a minor amount of polymerized surface vanadium oxide species on samples with high titania and vanadia loadings.

The UV−vis DRS spectral features of the hydrated $V_2O_5/TiO_2/SiO_2$ samples are dominated by the LMCT transitions of the hydrated surface vanadium oxide species, since these spectra are very similar to the hydrated V_2O_5/SiO_2 samples (see Figures 6 and 7). The ∼270 nm band is relatively stronger because of the contribution from the LMCT transitions of Ti cations in the $V_2O_5/TiO_2/SiO_2$ catalysts. As shown in Table 2, the edge energies of the hydrated $V_2O_5/TiO_2/SiO_2$ samples are far lower than these of the hydrated TiO_2/SiO_2 samples, indicating that these values are mainly determined by the edge energies of the hydrated surface vanadium oxide species. It was previously concluded[13] that the fully hydrated surface vanadium oxide species on silica consist of chain and/or 2D polymerized VO_5/VO_6 units. In comparison to the hydrated surface vanadium oxide species on pure silica, the presence of the titanium oxide species blue-shifts the LMCT bands and increases the edge energy of LMCT transitions by ∼0.2 eV (see Table 2), which suggests that the polymerization degree of VO_5/VO_6 polymers on these TiO_2/SiO_2 surfaces may be lower than on silica. The lower polymerization degree may be associated with the increase of the net pH at the point of zero charge (pzc) of the hydrated silica surface due to the addition of the somewhat more basic titanium oxide species.[17]

In the corresponding near-IR region (Figure 8), the 2ν overtone band of isolated Si−OH hydroxyls at 7315 cm^{-1} on the dehydrated TiO_2/SiO_2 and $V_2O_5/TiO_2/SiO_2$ samples are compared. The 7315 cm^{-1} band decreases significantly upon increasing either titania or vanadia loadings. It is noted that the addition of vanadium oxide on the 12% TiO_2/SiO_2 support at experimental monolayer coverage[10] consumes some of the remaining surface Si−OH hydroxyls that are inaccessible to the surface titanium oxide species, which suggests that the surface vanadium oxide species also interact with the silica surface. However, the relative amount of surface Si−OH hydroxyls consumed by the surface vanadium oxide species is less at a higher titania loading because of a lower concentration of the remaining Si−OH hydroxyls, indicative of a higher degree of interaction between the V cations and the surface titanium oxide species.

5. X-ray Absorption Spectroscopy (XANES). The Ti K-edge XANES spectra of the 15% TiO_2/SiO_2 and 10% V_2O_5/15% TiO_2/SiO_2 samples under hydrated and dehydrated conditions are presented in Figure 9. Compared to the Ti reference spectra reported previously,[10] the preedge peak position and height of the dehydrated 15% TiO_2/SiO_2 sample suggest that

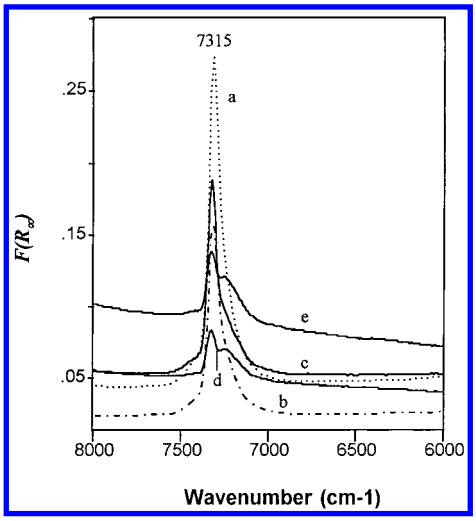

Figure 8. NIR DRS spectra of the dehydrated samples: (a) 5% TiO_2/SiO_2; (b) 12% TiO_2/SiO_2; (c) 5% V_2O_5/5% TiO_2/SiO_2; (d) 10% V_2O_5/5% TiO_2/SiO_2; (e) 10% V_2O_5/12% TiO_2/SiO_2.

the Ti atoms are predominantly 5-fold-coordinated. Hydration significantly decreases the preedge peak intensity and blue-shifts the peak position, indicating that the coordination number of the Ti atoms increases mostly to 6-fold. The addition of 10% V_2O_5 to the 15% TiO_2/SiO_2 support alters the coordination geometry of the Ti cations on the silica surface. The Ti preedge peak position and height of the hydrated and dehydrated 10% V_2O_5/15% TiO_2/SiO_2 sample indicate that the coordination of the Ti cations is predominantly 6-fold despite the different environmental conditions. The addition of surface vanadium oxide species appears to directly interact with surface titanium oxide species by binding to their unsaturated sites.

The V K-edge XANES spectra of the 10% V_2O_5/SiO_2 and 10% V_2O_5/15% TiO_2/SiO_2 sample under hydrated and dehydrated conditions are compared in Figure 10, and the corresponding energy positions of the main spectral features are summarized in Table 3. The preedge peak position and intensity of the 10% V_2O_5/15% TiO_2/SiO_2 sample are very close to those of the 10% V_2O_5/SiO_2 sample under the same environmental conditions. These results demonstrate that the surface V cations on the dispersed TiO_2/SiO_2 support possess a distorted VO_5 structure in the hydrated state and a distorted VO_4 structure in the dehydrated state, similar to the surface structures of the dispersed V_2O_5/SiO_2 catalyst under the same environmental conditions.[13]

6. Temperature-Programmed Reduction (TPR). TPR experiments were performed on the pure SiO_2, pure TiO_2, and dispersed TiO_2/SiO_2 supports to examine the reducibility of the supports. No noticeable H_2 consumption was observed for pure silica. Although the TPR spectra of TiO_2 and TiO_2/SiO_2 supports did not show noticeable H_2 consumption, these samples may have slight surface reduction because the sample color turned blue (Ti^{3+}) after a TPR run and the blue color quickly disappeared when the sample was exposed to air at room temperature. Therefore, the H_2 consumption detected for the various $V_2O_5/TiO_2/SiO_2$ catalysts shown below primarily originates from the reduction of the surface vanadium oxide species.

The TPR spectra of 1% V_2O_5 on pure SiO_2, pure TiO_2, and TiO_2/SiO_2 supports with various titania loadings are shown in Figure 11. The corresponding TPR results (i.e., the initial reduction temperature (T_{onset}), the maximum reduction temperature (T_{max}), the reduction peak width (fwhm), and the H_2 consumption represented by the H/V atomic ratio) are provided in Table 4. The T_{onset} decreases systematically with increasing titania loading, suggesting that the reducibility of some surface vanadium oxide species increases with increasing titania content. Surprisingly, the T_{max} values of the 1% $V_2O_5/x\%$ TiO_2/SiO_2 catalysts ($x\% \leq 15\%$) are significantly higher than that of 1% V_2O_5/SiO_2, suggesting that the modification of silica by the surface titanium oxide species seems to decrease the reducibility of the majority of surface vanadium oxide species and that a strong interaction exists between the surface vanadium oxide and surface titanium oxide species. Furthermore, the decreased reducibility of the surface vanadium oxide species on TiO_2/SiO_2 in comparison to V_2O_5/SiO_2 suggests that the surface titanium oxide species must possess very different chemical properties from crystalline TiO_2 (anatase). It can be seen that the reduction peak becomes significantly broader with increasing titania loading from 0% to 15% TiO_2, and then the TPR spectrum splits into two reduction peaks for the 1% V_2O_5/30% TiO_2/SiO_2 sample where both TiO_2 crystallites and the surface titanium oxide species coexist on silica. At a higher loading of 50% TiO_2, only one reduction peak at 463 °C due to the reduction of surface vanadium oxide species on the crystalline TiO_2 is observed, suggesting that only the crystalline TiO_2 is present on silica at this high titania loading. The 1% V_2O_5/TiO_2 sample also exhibits one reduction peak at 435 °C, which is much lower than all the $V_2O_5/TiO_2/SiO_2$ catalysts.

The TPR results of 5% V_2O_5 on various supports are listed in Table 5, and some of the TPR spectra are shown in Figure 12. The peak width increases with titania loading up to 30% TiO_2 and then decreases at 50% TiO_2. The T_{onset} values of these catalysts decrease systematically with increasing titania loading, whereas the T_{max} values of the dispersed 5% $V_2O_5/x\%$ TiO_2/SiO_2 catalysts ($x\% \leq 15\%$) shift upward in comparison with the 5% V_2O_5/SiO_2 sample, indicating that the surface vanadium oxide species, when associated with the surface titanium oxide species, possess different reducibility from crystalline TiO_2. The fact that the 5% V_2O_5/50% TiO_2/SiO_2 sample still exhibits a much lower reducibility than the 5% V_2O_5/TiO_2 sample suggests that the influence of SiO_2 as a substrate may still play a role in the catalyst.

The TPR results of 10% V_2O_5 on various supports are provided in Table 6. In contrast to the lower vanadia loading samples (1% and 5% V_2O_5), both T_{max} and T_{onset} of the 10% $V_2O_5/TiO_2/SiO_2$ catalysts systematically decrease with increasing titania loading from 0% to 30% TiO_2. It appears that at the 1% V_2O_5 loading, the distribution of different surface vanadium oxide species on the TiO_2/SiO_2 support is more pronounced as recognized from the broad reduction peak and the peak splitting at 30% TiO_2. However, at the 10% V_2O_5 loading, the reduction of a large quantity of the surface vanadium oxide species may result in the loss of the detailed structural information about the distribution of different surface vanadium oxide species on the TiO_2/SiO_2 support. Moreover, the detailed reduction mechanism and the influence of the modification of support on the reduction process are not very clear at the present time.

It can be seen from Tables 4−6 that the H/V ratios for 5% and 10% V_2O_5 on various supports are almost constant at ~2, which shows that the average oxidation state of the V cations after TPR reduction up to 700 °C is about +3. The H/V ratios for 1% V_2O_5 on all the TiO_2/SiO_2 supports are higher than 2, but these values are not very reliable considering that the signal-to-noise ratio is very low and the reduction peaks are very broad. In all cases (see Tables 4−6), the surface vanadium oxide species on TiO_2/SiO_2 show broader peak widths than on pure SiO_2 and on pure TiO_2, and the maximum peak width is observed for the surface vanadium oxide species on 30 wt %

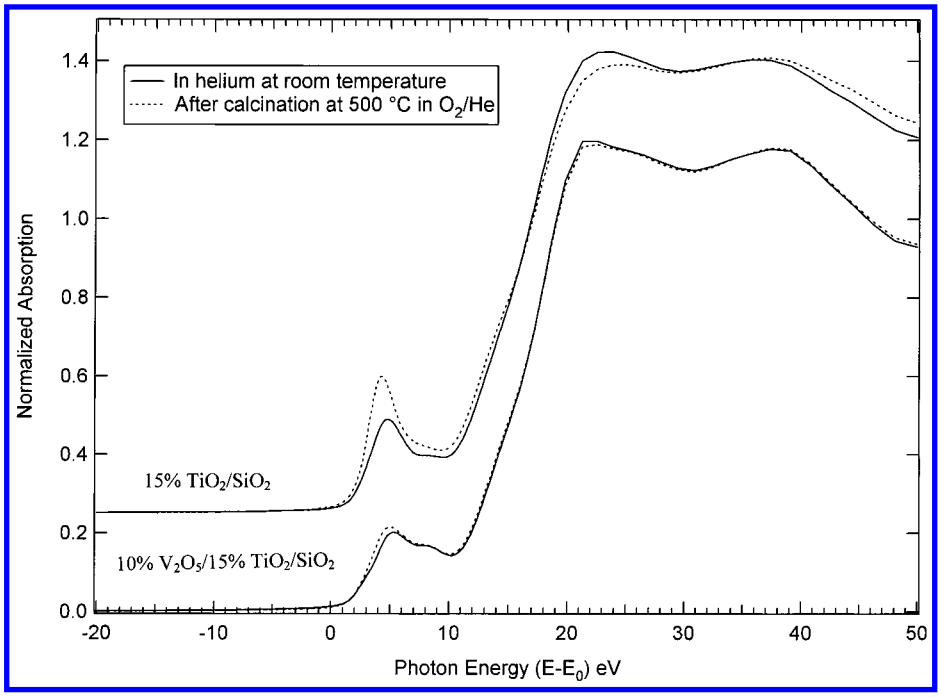

Figure 9. Ti K-edge XANES spectra of the 15% TiO_2/SiO_2 and 10% V_2O_5/15% TiO_2/SiO_2 samples under hydrated (solid lines) and dehydrated (dash lines) conditions.

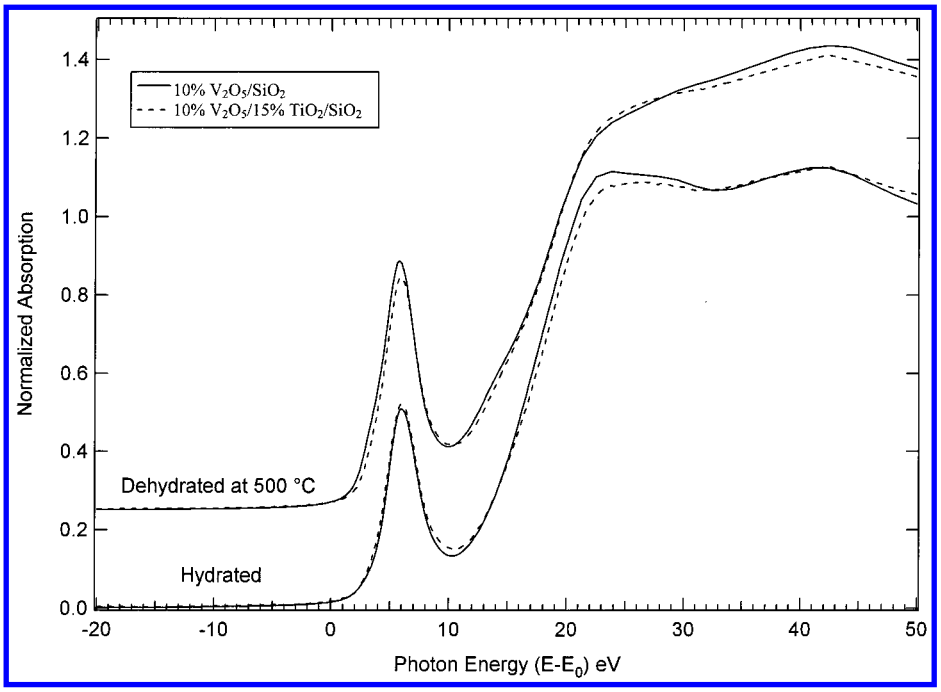

Figure 10. V K-edge XANES spectra of the 10% V_2O_5/SiO_2 (solid lines) and 10% V_2O_5/15% TiO_2/SiO_2 samples (dash lines) under hydrated and dehydrated conditions.

TiO_2, suggesting that more than one type of the surface vanadium oxide species are present (e.g., the surface vanadium oxide species that are associated with the dispersed titanium oxide species and the surface vanadium oxide species that are associated with crystalline TiO_2).

The TPR spectra of the fresh 5% V_2O_5 on various supports and the reoxidized samples after the TPR runs are compared in Figure 12, and the corresponding results are also listed in Table 5. The 5% V_2O_5/SiO_2 sample is relatively stable after a redox cycle, since, except for a slight upward shift of the T_{max}, no obvious change is observed on the peak width and the H/V ratio. In contrast, the 5% V_2O_5/TiO_2 sample is not stable after the redox cycle because the H_2 consumption significantly decreases and the reduction peak becomes broader in the second TPR run. This result suggests that the surface area of the catalyst may greatly be reduced after a TPR run up to 700 °C and some V(V) atoms probably migrate into the TiO_2 support that are stabilized at a lower valence state, most likely V(IV) cations.[18] The surface vanadium oxide species on TiO_2/SiO_2 supports are relatively stable, especially on the surface titanium oxide modified silica supports, since the peak width and H_2 consumption are essentially unchanged after the redox cycle for these catalysts.

7. Methanol Oxidation. Methanol oxidation was employed to examine the catalytic properties of the $V_2O_5/TiO_2/SiO_2$ catalysts. The silica did not show any noticeable activity for methanol oxidation under the present experimental conditions.

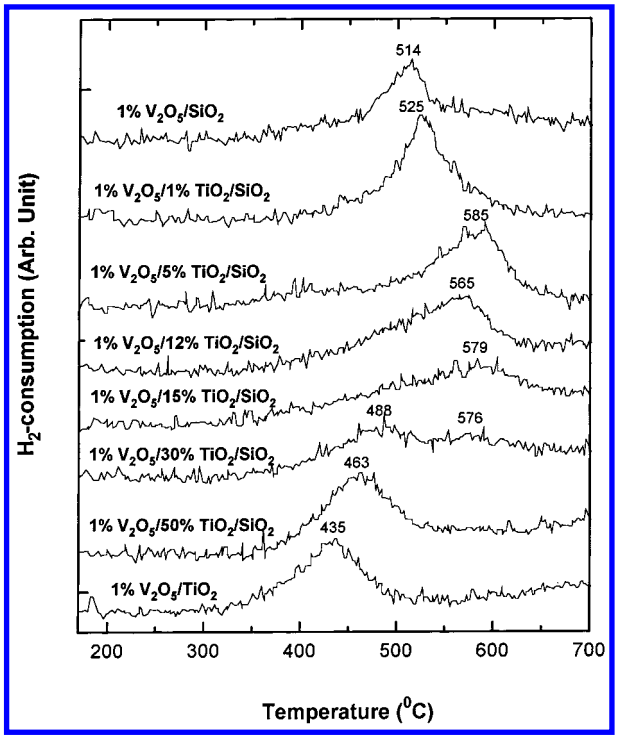

Figure 11. TPR profiles of 1% V_2O_5 on various supports.

TABLE 4: TPR Results for 1% V_2O_5 on Various Supports[a]

sample	T_{onset} (°C)	T_{max} (°C)	fwhm (°C)	H/V (atomic ratio)
1% V_2O_5/SiO_2	396	514	40	1.87
1% V_2O_5/1% TiO_2/SiO_2	394	525	50	2.88
1% V_2O_5/5% TiO_2/SiO_2	383	585	76	2.78
1% V_2O_5/12% TiO_2/SiO_2	361	565	100	3.13
1% V_2O_5/15% TiO_2/SiO_2	365	579	122	2.42
1% V_2O_5/30% TiO_2/SiO_2	361	488, 576		2.53
1% V_2O_5/50% TiO_2/SiO_2	365	463	76	2.52
1% V_2O_5/TiO_2	321	435	62	1.98

[a] Sample weight ≈ 60 mg; temperature rate = 10 °C/min.

TABLE 5: TPR Results for the Fresh and Reoxidized 5% V_2O_5 on Various Supports[a]

sample	T_{onset} (°C)	T_{max} (°C)	fwhm (°C)	H/V (atomic ratio)
5% V_2O_5/SiO_2	383	526	40	1.88
reoxidized	386	534	39	1.90
5% V_2O_5/1% TiO_2/SiO_2	383	532	42	2.06
5% V_2O_5/5% TiO_2/SiO_2	378	537	58	1.95
reoxidized	379	544	60	1.94
5% V_2O_5/12% TiO_2/SiO_2	364	538	77	2.13
5% V_2O_5/15% TiO_2/SiO_2	354	530	91	2.05
reoxidized	343	530	98	2.04
5% V_2O_5/30% TiO_2/SiO_2	338	498	94	2.08
reoxidized	334	496	102	1.91
5% V_2O_5/50% TiO_2/SiO_2	337	494	77	2.03
5% V_2O_5/TiO_2	315	456	62	2.01
reoxidized	315	472	71	1.69

[a] Sample weight ≈ 60 mg; temperature rate = 10 °C/min.

The catalytic results of the TiO_2/SiO_2 supported oxides for methanol oxidation at 270 °C are presented in Table 7 for comparison. The catalytic results of the surface vanadium oxide species on SiO_2, TiO_2, and TiO_2/SiO_2 for methanol oxidation at 270 °C are provided in Table 8. All the catalysts exhibit high selectivities to redox products (>95%). The activity of the 1% V_2O_5/SiO_2 sample at 270 °C is very low (TOF ≈ 10^{-3} s^{-1}). In contrast, the TOF for the 1% TiO_2/SiO_2 samples at 270 °C is nearly 1 order of magnitude (TOF ≈ 10^{-2} s^{-1}) higher than that

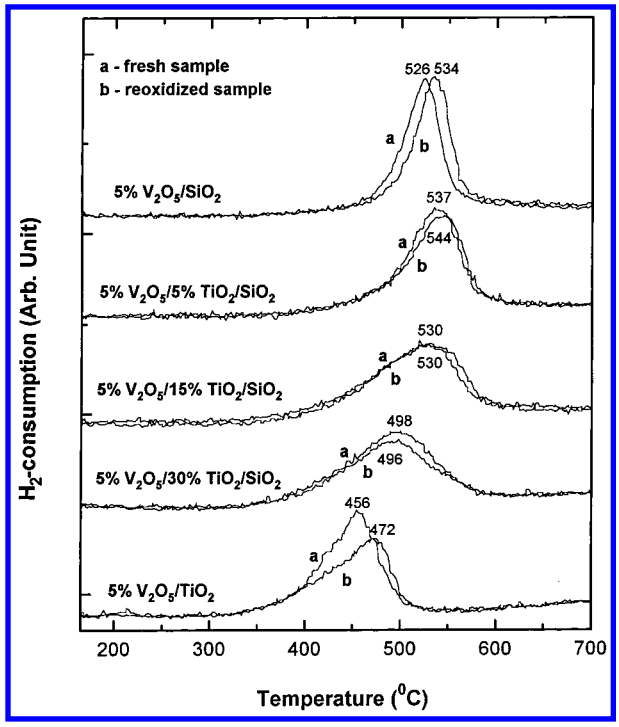

Figure 12. Comparison of TPR profiles of fresh and reoxidized 5% V_2O_5 on various supports.

TABLE 6: TPR Results for 10% V_2O_5 on Various Supports[a]

sample	T_{onset} (°C)	T_{max} (°C)	fwhm (°C)	H/V (atomic ratio)
10% V_2O_5/SiO_2	390	540	38	2.00
10% V_2O_5/1% TiO_2/SiO_2	370	531	44	2.07
10% V_2O_5/5% TiO_2/SiO_2	344	530	56	1.94
10% V_2O_5/12% TiO_2/SiO_2	346	528	68	2.00
10% V_2O_5/15% TiO_2/SiO_2	338	520	80	2.09
10% V_2O_5/30% TiO_2/SiO_2	339	507	90	1.92

[a] Sample weight ≈ 60 mg; temperature rate = 10 °C/min.

TABLE 7: Activity/Selectivity of TiO_2/SiO_2 Catalysts for Methanol Oxidation at 270 °C

catalyst	Ac[a] (mmol g^{-1} h^{-1})	TOF[b] (10^{-3} s^{-1})	selectivity (%) HCHO	MF	DMM	DME
1% TiO_2/SiO_2	16	35	68	32	0	0
5% TiO_2/SiO_2	28	12	59	39	2	0
8% TiO_2/SiO_2	15	4	65	32	3	0
12% TiO_2/SiO_2	12	2	68	28	4	0
30% TiO_2/SiO_2	3					

[a] Millimoles of methanol converted per gram catalyst per hour. [b] TOF is calculated on the basis of the total Ti atoms in the catalysts for the production of HCHO (formaldehyde) + MF (methyl formate) + DMM (dimethoxymethane).

of the 1% V_2O_5/SiO_2 sample, demonstrating that the isolated TiO_4 species on silica possess a higher reactivity for methanol oxidation than the isolated VO_4 species on silica. However, the addition of 1% V_2O_5 onto the 1% TiO_2/SiO_2 sample greatly reduces the overall activity (4 times less active), suggesting that the surface vanadium oxide species directly interact with the surface titanium oxide species. Also, the addition of 1% V_2O_5 onto the 5% TiO_2/SiO_2 support decreases slightly the overall activity. It is not clear for the dispersed $V_2O_5/TiO_2/SiO_2$ catalysts, especially 1% V_2O_5/1% TiO_2/SiO_2 and 1% V_2O_5/5% TiO_2/SiO_2 samples, whether some Ti(IV) cations might still serve as the active sites for methanol oxidation. However, the

TABLE 8: Activity and Selectivity of V_2O_5/SiO_2, $V_2O_5/TiO_2/SiO_2$, and V_2O_5/TiO_2 Catalysts for Methanol Oxidation at 270 °C

catalyst	E_a (kcal mol^{-1})	Ac (mmol g^{-1} h^{-1})	TOF[a] (10^{-3} s^{-1})	selectivity (%) HCHO	MF	DMM	DME
1% V_2O_5/SiO_2		1	2				
1% V_2O_5/1% TiO_2/SiO_2		4	10				
1% V_2O_5/5% TiO_2/SiO_2	17.9	21	52	82	15	3	0
1% V_2O_5/8% TiO_2/SiO_2		23	57	85	5	6	4
1% V_2O_5/12% TiO_2/SiO_2		30	72	85	5	6	4
1% V_2O_5/30% TiO_2/SiO_2	21	57	140	89	1	7	3
1% V_2O_5/50% TiO_2/SiO_2	20.9	170	420	87	7	4	2
1% V_2O_5/TiO_2	15.9	297	750	93	5	2	0
5% V_2O_5/5% TiO_2/SiO_2	19.8	46	23	82	12	4	2
5% V_2O_5/8% TiO_2/SiO_2		99	49	85	10	2	3
5% V_2O_5/12% TiO_2/SiO_2	19.4	112	55	81	10	6	3
10% V_2O_5/5% TiO_2/SiO_2	17.2	55	14	83	14	3	0
10% V_2O_5/12% TiO_2/SiO_2		300	74	91	5	2	2

[a] TOF is calculated on the basis of the total V atoms in the catalysts for the production of HCHO (formaldehyde) + MF (methyl formate) + DMM (dimethoxymethane).

selectivity pattern of these 1% $V_2O_5/TiO_2/SiO_2$ catalysts (the selectivity of HCHO is >80%) is different from that of TiO_2/SiO_2 supports (the selectivity of HCHO is <70%), which suggests that the surface vanadium oxide species play a major role as the active sites for methanol oxidation.

Comparison of the catalytic activity (TOF) of 1% V_2O_5 as a function of the support is very informative. As can be seen in Table 8, the modification of silica by titanium oxide significantly enhances the reactivity of the catalysts. For the dispersed TiO_2/SiO_2 with relatively high concentrations of surface titanium oxide species (5% TiO_2 ≤ titania loading ≤ 15% TiO_2), the activity is more than an order of magnitude higher than that of the V_2O_5/SiO_2 catalyst. However, the presence of crystalline TiO_2 on silica (i.e., 30% TiO_2/SiO_2 and 50% TiO_2/SiO_2) can enhance the TOF of the surface vanadium oxide species by 2 orders of magnitude relative to the V_2O_5/SiO_2 catalyst. Notably, all the TiO_2/SiO_2 supports are less effective than pure TiO_2 as the support for vanadium oxide for methanol oxidation, which may be due to the influence from the silica substrate and/or due to the fact that the TiO_2 particle size on silica is smaller than pure TiO_2.

It is interesting to note from Table 8 that the TOF of the surface vanadium oxide species on 12% TiO_2/SiO_2, which is at monolayer coverage of surface titanium oxide species, is almost constant at various vanadia loadings. However, below monolayer coverage of surface titanium oxide on silica, such as 5% TiO_2/SiO_2, increasing the vanadia loading decreases the TOF, indicative of the decreased interaction between the surface vanadium oxide and titanium oxide species. With the same vanadia loading, the TOF systematically increases with titania loading, indicative of the increased interaction between the surface vanadium oxide and titanium oxide species. The activation energy E_a of various $V_2O_5/TiO_2/SiO_2$ catalysts is 17−21 kcal/mol, which is within the range of methanol oxidation over supported vanadium oxide catalysts[19] and other transition-metal oxide catalysts,[20] suggesting that a similar reaction mechanism is operating over all these metal oxide catalysts.

Discussions

Structural Characteristics of the Dispersed $V_2O_5/TiO_2/SiO_2$ Catalysts. The in situ Raman, UV−vis−NIR DRS, and XANES spectroscopies indicate that the surface vanadium oxide species on the dispersed TiO_2/SiO_2 supports are sensitive to the environmental conditions. In the dehydrated state, the edge energies of the LMCT transitions for the dispersed $V_2O_5/TiO_2/SiO_2$ catalysts are very close to that of the dispersed V_2O_5/SiO_2. The Raman spectra of the dispersed $V_2O_5/TiO_2/SiO_2$ catalysts are also very similar to the dispersed V_2O_5/SiO_2. In addition, the V K-edge XANES experiments show that the coordination of the V cations on TiO_2/SiO_2 is 4-fold, similar to the surface V cations on SiO_2. All the above experimental results suggest that the molecular structure of the surface vanadium oxide species on the dispersed TiO_2/SiO_2 supports is predominantly isolated VO_4 units (i.e., O═V(O−support)$_3$ group), which is similar to the surface vanadium oxide species on pure silica. This conclusion is also supported by the ^{51}V NMR spectroscopic study of the dispersed 7% V_2O_5/10% TiO_2/SiO_2 sample,[21] which shows that the dehydrated surface vanadium oxide species are predominately tetrahedral VO_4 species.

In the hydrated state, the Raman spectra of the dispersed $V_2O_5/TiO_2/SiO_2$ catalysts are also very similar to the dispersed V_2O_5/SiO_2. In addition, the UV−vis DRS results indicate that the hydrated surface vanadium oxide species on the dispersed TiO_2/SiO_2 supports are 2D polymerized VO_5/VO_6 units but with a lower degree of polymerization than the hydrated vanadium oxide species on pure silica because of the presence of the somewhat more basic titanium oxide species. However, the catalysts are usually in the dehydrated state during methanol oxidation as well as in the TPR studies. Therefore, the structural characteristics of the catalysts in the dehydrated state are more relevant to the chemical and catalytic properties of the catalysts. Consequently, only the dehydrated molecular structures of the $V_2O_5/TiO_2/SiO_2$ catalysts are discussed below.

Although the modification of silica by surface titanium oxide species does not affect molecular structures of the dispersed vanadium oxide species (still isolated VO_4 units), the molecular structure of the dispersed titanium oxide species is greatly affected by the presence of the dispersed vanadium oxide species. The XANES experiments indicate that the deposition of vanadium oxide increases the coordination number of the dispersed Ti cations by saturating their coordination sites. These results suggest the direct interaction between surface vanadium oxide species and surface titanium oxide species.

The direct interaction between the surface vanadium oxide species and titanium oxide species is further confirmed by Raman spectroscopy. The two new Raman bands at 648−637 and ∼248 cm^{-1}, which are tentatively assigned to the stretching and bending modes of the V−O−Ti bridging bonds, are due to the interaction between the two surface layers at relatively high vanadia and titania loadings on silica. However, the simultaneous disappearance of the Raman band at 607 cm^{-1} due to the silica vibration strongly suggests that the surface vanadium

oxide species also interact with silica. NIR DRS experiments reveal that the deposition of vanadium oxide on TiO_2/SiO_2 also consumes the surface Si−OH hydroxyls, indicative of the formation of V−O−Si bridging bonds. It is not clear from the Raman and DRS results whether an isolated VO_4 unit possesses only three oxygenated Si(IV)−O^- ligands or only three Ti(IV)−O^- ligands or a simultaneous combination of both types of ligands. However, it was found that all the TPR peaks observed for the dispersed $V_2O_5/TiO_2/SiO_2$ catalysts are broad and unresolvable, suggesting that although the surface vanadium oxide species are predominantly isolated VO_4 units, different types of V(V) sites may coexist on the TiO_2/SiO_2 surface, e.g., V(V) sites with different Ti(IV)−O^- to Si(IV)−O^- ligand ratios (from 3:0 to 0:3).

The above characterization results indicate that the dispersed $V_2O_5/TiO_2/SiO_2$ catalysts synthesized in the present study possess both surface vanadium oxide and titanium oxide species on silica and that the two surface metal oxide species directly interact with each other. The direct interaction between the two surface layers constitutes the bilayered surface metal oxides on silica, which is defined as a bilayered surface metal oxide catalyst.

Fundamental Relationships between Structural Characteristics and Catalytic Properties of the Dispersed $V_2O_5/TiO_2/SiO_2$ Catalysts. The catalytic results show that even far below the monolayer coverage for either vanadium oxide or titanium oxide, the addition of 1% V_2O_5 onto the 1% TiO_2/SiO_2 sample greatly reduces the overall activity (4 times less active), further suggesting a direct interaction between the surface vanadium oxide and titanium oxide species. The dehydrated 1% TiO_2/SiO_2 sample consists of isolated TiO_4 units. The presence of the isolated VO_4 groups affects the catalytic behavior of the surface titanium oxide species on silica by most probably altering the coordination geometry of the Ti cations, which apparently decreases the oxidation potentials of the Ti cations. A similar phenomenon has been found in titanosilicate mesoporous TiMCM-41 molecular sieves where isolated framework Ti cations can immobilize surface vanadium cations and promote the oxidation of V(IV) to V(V).[22]

Although the molecular structure of the dehydrated surface vanadium oxide species on the TiO_2/SiO_2 supports is essentially the same as that of the dispersed V_2O_5/SiO_2 catalysts, the change of the oxygenated ligands greatly affects the catalytic properties of the surface V cations. The TOFs for methanol oxidation on the dispersed $V_2O_5/TiO_2/SiO_2$ supports are an order of magnitude greater than the V_2O_5/SiO_2 catalysts. In situ Raman studies of the dispersed 10% V_2O_5/12% TiO_2/SiO_2 catalyst demonstrate that the surface V−methoxy complexes formed on 12% TiO_2/SiO_2 are similar to the complexes on pure TiO_2. For the 5% V_2O_5/5% TiO_2/SiO_2 catalyst, in situ Raman studies also demonstrate that during methanol oxidation, the surface vanadium oxide species behave more like such species on TiO_2 than on SiO_2. These results suggest that the active V sites on TiO_2/SiO_2 supports are preferentially coordinated to the surface titanium oxide species. This is further confirmed by the temperature-programmed-reaction spectroscopy (TPRS) studies of methanol oxidation.[23] The TPRS studies show that the decomposition temperature of the surface V−methoxy species to formaldehyde on TiO_2/SiO_2 is the same as on pure TiO_2 (220 °C) and is significantly lower than on pure silica (284 °C). The replacement of the Si(IV)−O^- ligand by the Ti(IV)−O^- ligand in the coordination sphere of the V cation enhances the decomposition of the surface V−methoxy species, indicating that the most active sites for surface methoxy decomposition are surface VO_x sites coordinated to Ti cations. Therefore, the presence of V−O−Ti bonds in the isolated vanadium oxide species on the TiO_2/SiO_2 support is responsible for the enhanced reactivity of the surface V active sites.

Furthermore, the TOF of the surface vanadium oxide species on 12% TiO_2/SiO_2 at monolayer coverage is almost constant at various vanadia loadings. However, the V═O stretching vibration varies from 1033 to 1038 cm^{-1} (see Figure 1), which indicates an increase in the V═O bond strength.[15] Thus, it appears that no relationship exists between the V═O bond strength and the reactivity of the catalysts.

The basis for the reactivity enhancement of the isolated VO_4 sites upon coordination to the Ti cation may lie in the increase of the electron density of the bridging oxygen of the V−O− support bond, since the Ti(IV) cations possess a lower electronegativity than the Si(IV) cations.[24] However, the electronegativity of the Ti(IV) cations that interact with both silica and vanadium oxide species should be higher than that of Ti(IV) in pure TiO_2 because of the higher electron-withdrawing ability of Si(IV) and V(V) cations. This is further confirmed by the increased BE values of Ti $2p_{3/2}$ in the dispersed $V_2O_5/TiO_2/SiO_2$ catalysts. Therefore, the influence of silica as the substrate reduces the electron density on the V−O−Ti bridging bonds, which decreases the reactivity of the surface V sites during methanol oxidation relative to V_2O_5/TiO_2.

The isolated V(V) sites on the dispersed TiO_2/SiO_2 supports may have some potential applications in the partial oxidation of hydrocarbons, since it has been suggested[25] that the dispersed, isolated redox sites would be more selective for selective partial oxidation reactions due to the lower availability of oxygen atoms for total oxidation. Some preliminary results have demonstrated that the bilayered $V_2O_5/TiO_2/SiO_2$ catalysts are very selective for partial oxidation of ethane to ethylene.[26]

Conclusions

The surface structures of dispersed and bilayered $V_2O_5/TiO_2/SiO_2$ catalysts under various conditions (e.g., hydrated, dehydrated, and methanol oxidation conditions) were extensively investigated by combined in situ Raman and UV−vis−NIR DRS and XANES spectroscopy, as well as XPS. The characterization studies revealed that the surface structures of the dispersed $V_2O_5/TiO_2/SiO_2$ catalysts are a strong function of environmental conditions. The surface vanadium oxide species on the dispersed TiO_2/SiO_2 supports are predominantly isolated VO_4 units in the dehydrated state and become polymerized VO_5/VO_6 units upon hydration. The surface V cations preferentially interact with the surface titanium oxide species on silica. Consequently, the coordination of the surface Ti cations increases and the reducibility and catalytic properties of the surface vanadium oxide species are significantly altered. In the dehydrated state, the V(V) cations appear to possess both oxygenated ligands of Si(IV)−O^- and Ti(IV)−O^- with varying ratios from 3:0 to 0:3, which depend on vanadia and titania loadings. In situ Raman studies demonstrated that the intermediate surface V−methoxy complexes formed on TiO_2/SiO_2 are similar to those on TiO_2 rather than on SiO_2. As a result of the interaction between the surface vanadium oxide and titanium oxide species on silica, the TOF of the surface VO_4 species for methanol oxidation increases by more than an order of magnitude relative to V_2O_5/SiO_2. This reactivity enhancement is associated with the change of the Si(IV)−O^- oxygenated ligands by less electronegative Ti(IV)−O^- ligands. However, no apparent correlation was found between the TPR reducibility and methanol oxidation reactivity of the $V_2O_5/TiO_2/SiO_2$ catalysts.

Acknowledgment. This work was funded by the U.S. National Science Foundation Grant CTS-9417981. The UV−vis−NIR DRS experiments were performed on a Varian Cary 5 UV−vis−NIR spectrometer that was supported by the U.S. Department of Energy−Basic Energy Sciences, Grant DE-FG02-93ER14350. Part of the research was carried out at the National Synchrotron Light Source, Brookhaven National Laboratory, which is supported by the U.S. Department of Energy, Division of Materials Sciences and Division of Chemical Sciences. The authors thank Dr. Miguel A. Banares for the help with BET measurements and chemical analysis.

References and Notes

(1) Mariscal, R.; Galan-Fereres, M.; Anderson, J. A.; Alemany, L. J.; Palacios, J. M.; Fierro, J. L. G. *Environmental Catalysis*; Centi, G., et al., Eds.; SCI: Rome, 1995; p 223.

(2) Amiridis, M. D.; Solar, J. P. *Ind. Eng. Chem. Res*. **1996**, *35*, 978.

(3) (a) Rajadhyaksha, R. A.; Hausinger, G.; Zeilinger, H.; Ramstetter, A.; Schmeiz, H.; Knözinger, H. *Appl. Catal*. **1989**, *51*, 67. (b) Rajadhyaksha, R. A.; Knözinger, H. *Appl. Catal*. **1989**, *51*, 81.

(4) Wauthoz, P.; Machej, T.; Grange, P. *Appl. Catal*. **1991**, *69*, 149.

(5) Vogt, E. T. C.; Boot, A.; van Dillen, A. J.; Geus, J. W.; Janssen, F. J. J. G.; van den Kerkhof, F. M. G. *J. Catal*. **1988**, *114*, 313.

(6) Galan-Fereres, M.; Mariscal, R.; Alemany, L. J.; Fierro, J. L. G. *J. Chem. Soc., Faraday Trans*. **1994**, *90*, 3711.

(7) Elguezabal, A. A.; Corberan, V. C. *Catal. Today* **1996**, *32*, 265.

(8) (a) Dias, C. R.; Portela, M. F.; Galan-Fereres, M.; Banares, M. A.; Granados, M. L.; Pena, M. A.; Fierro, J. L. G. *Catal. Lett*. **1997**, *43*, 117. (b) Quaranta, N. E.; Soria, J.; Corberan, V. C.; Fierro, J. L. G. *J. Catal.* **1997**, *171*, 1.

(9) Lapina, O. B.; Mastikhin, V. M.; Dubkov, K. A.; Mokrinski, V. V. *J. Mol. Catal*. **1994**, *87*, 57.

(10) Gao, X.; Bare, S. R.; Fierro, J. L. G.; Banares, M. A.; Wachs, I. E. *J. Phys. Chem. B* **1998**, *102*, 5653.

(11) Jehng, J. M.; Hu, H.; Gao, X.; Wachs, I. E. *Catal. Today* **1996**, *28*, 335.

(12) Delgass, W. N.; Haller, G. L.; Kellerman, R.; Lunsford, J. H. *Spectroscopy in Heterogeneous Catalysis*; Academic Press: New York, 1979.

(13) Gao, X.; Bare, S. R.; Weckhuysen, B. M.; Wachs, I. E. *J. Phys. Chem*., in press.

(14) Wachs, I. E.; Deo, G.; Weckhuysen, B. M.; Andreini, A.; Vuurman, M. A.; de Boer, M.; Amiridis, M. D. *J. Catal*. **1996**, *161*, 211.

(15) Hardcastle, F.; Wachs, I. E. *J. Phys. Chem*. **1991**, *95*, 5031.

(16) Busca, G.; Elmi, A. S.; Forzatti, P. *J. Phys. Chem*. **1980**, *73*, 3274.

(17) Deo, G.; Wachs, I. E. *J. Phys. Chem*. **1991**, *95*, 5889.

(18) Banares, M. A.; Alemany, L. J.; Jimenez, M. C.; Larrubia, M. A.; Delgado, F.; Granados, M. L.; Martinez-Arias, A.; Blasco, J. M.; Fierro, J. L. G. *J. Solid State Chem*. **1996**, *124*, 69.

(19) Deo, G.; Wachs, I. E. *J. Catal*. **1994**, *146*, 323.

(20) Weber, R. S. *J. Phys. Chem*. **1994**, *98*, 2999.

(21) Lapina, O. B.; Nosov, A. V.; Hu, H.; Wachs, I. E. Unpublished results.

(22) Luan, Z.; Kevan, L. *J. Phys. Chem. B* **1997**, *101*, 2020.

(23) Juskelis, M.; Wachs, I. E. Unpublished results.

(24) Sanderson, R. T. *J. Chem. Educ*. **1988**, *65*, 113.

(25) Kung, H.; Kung, M. C. *Catal. Today* **1996**, *30*, 5.

(26) Banares, M.; Gao, X.; Fierro, J. L. G.; Wachs, I. E. *Stud. Surf. Sci. Catal.* **1997**, *110*, 295.